Therapeutic efficacy of the small molecule GS-5734 against Ebola virus in rhesus monkeys

Travis K. Warren[1,2], Robert Jordan[3], Michael K. Lo[4], Adrian S. Ray[3], Richard L. Mackman[3], Veronica Soloveva[1,2], Dustin Siegel[3], Michel Perron[3], Roy Bannister[3], Hon C. Hui[3], Nate Larson[3], Robert Strickley[3], Jay Wells[1], Kelly S. Stuthman[1], Sean A. Van Tongeren[1], Nicole L. Garza[1], Ginger Donnelly[1], Amy C. Shurtleff[1], Cary J. Retterer[1], Dima Gharaibeh[1], Rouzbeh Zamani[1], Tara Kenny[1], Brett P. Eaton[1], Elizabeth Grimes[1], Lisa S. Welch[1]†, Laura Gomba[1,2], Catherine L. Wilhelmsen[1], Donald K. Nichols[1], Jonathan E. Nuss[1,2], Elyse R. Nagle[1], Jeffrey R. Kugelman[1], Gustavo Palacios[1], Edward Doerffler[3], Sean Neville[3], Ernest Carra[3], Michael O. Clarke[3], Lijun Zhang[3], Willard Lew[3], Bruce Ross[3], Queenie Wang[3], Kwon Chun[3], Lydia Wolfe[3], Darius Babusis[3], Yeojin Park[3], Kirsten M. Stray[3], Iva Trancheva[3], Joy Y. Feng[3], Ona Barauskas[3], Yili Xu[3], Pamela Wong[3], Molly R. Braun[5], Mike Flint[4], Laura K. McMullan[4], Shan-Shan Chen[3], Rachel Fearns[5], Swami Swaminathan[3], Douglas L. Mayers[1]†, Christina F. Spiropoulou[4], William A. Lee[3], Stuart T. Nichol[4], Tomas Cihlar[3] & Sina Bavari[1,2]

The most recent Ebola virus outbreak in West Africa, which was unprecedented in the number of cases and fatalities, geographic distribution, and number of nations affected, highlights the need for safe, effective, and readily available antiviral agents for treatment and prevention of acute Ebola virus (EBOV) disease (EVD) or sequelae[1]. No antiviral therapeutics have yet received regulatory approval or demonstrated clinical efficacy. Here we report the discovery of a novel small molecule GS-5734, a monophosphoramidate prodrug of an adenosine analogue, with antiviral activity against EBOV. GS-5734 exhibits antiviral activity against multiple variants of EBOV and other filoviruses in cell-based assays. The pharmacologically active nucleoside triphosphate (NTP) is efficiently formed in multiple human cell types incubated with GS-5734 *in vitro*, and the NTP acts as an alternative substrate and RNA-chain terminator in primer-extension assays using a surrogate respiratory syncytial virus RNA polymerase. Intravenous administration of GS-5734 to nonhuman primates resulted in persistent NTP levels in peripheral blood mononuclear cells (half-life, 14 h) and distribution to sanctuary sites for viral replication including testes, eyes, and brain. In a rhesus monkey model of EVD, once-daily intravenous administration of 10 mg kg^{-1} GS-5734 for 12 days resulted in profound suppression of EBOV replication and protected 100% of EBOV-infected animals against lethal disease, ameliorating clinical disease signs and pathophysiological markers, even when treatments were initiated three days after virus exposure when systemic viral RNA was detected in two out of six treated animals. These results show the first substantive post-exposure protection by a small-molecule antiviral compound against EBOV in nonhuman primates. The broad-spectrum antiviral activity of GS-5734 *in vitro* against other pathogenic RNA viruses, including filoviruses, arenaviruses, and coronaviruses, suggests the potential for wider medical use. GS-5734 is amenable to large-scale manufacturing, and clinical studies investigating the drug safety and pharmacokinetics are ongoing.

The 2013–2016 outbreak of EVD in West Africa was the largest and most complex EBOV outbreak in the recorded history of the disease, with >28,000 EVD cases and >11,000 reported deaths[1]. Medical infrastructures in Guinea, Sierra Leone, and Liberia were seriously impacted by a loss of >500 healthcare workers[1]. Additionally, EVD-related sequelae (joint and muscle pain, as well as neurological, ophthalmic, and other symptoms) together with viral persistence and recrudescence in individuals who survived the acute disease have been documented[2–5].

EBOV is a single-stranded negative-sense non-segmented RNA virus from the *Filoviridae* family. In addition to EBOV, other related viruses, namely Marburg, Sudan, and Bundibugyo viruses, have caused outbreaks with high fatality rates[6]. Although the efficacy of various experimental small molecules and biologics have been assessed in EVD animal models and in multiple clinical trials during the West African outbreak[7–18], there are no therapeutics for which clinical efficacy and safety have been established for treatment of acute EVD or its sequelae. The availability of broadly effective antiviral(s) with a favourable benefit/risk profile would address a serious unmet medical need for the treatment of EBOV infection.

A 1′-cyano-substituted adenine C-nucleoside ribose analogue (Nuc) exhibits antiviral activity against a number of RNA viruses[19]. The mechanism of action of Nuc requires intracellular anabolism to the active triphosphate metabolite (NTP), which is expected to interfere with the activity of viral RNA-dependent RNA-polymerases (RdRp). Structurally, the 1′-cyano group provides potency and selectivity towards viral RNA polymerases, but because of slow first phosphorylation kinetics, modification of parent nucleosides with monophosphate promoieties has the potential to greatly enhance intracellular NTP concentrations[20]. GS-5734, the single *S*p isomer of the 2-ethylbutyl L-alaninate phosphoramidate prodrug (Supplementary Information), effectively bypasses the rate-limiting first phosphorylation step of the Nuc (Fig. 1a). In human monocyte-derived macrophages, incubation with GS-5734 caused rapid loading of cells with high levels of NTP that persist with a half-life ($t_{1/2}$) of 24 h following removal of GS-5734 (Extended Data Fig. 1a), resulting in up to 30-fold higher levels compared to incubation with Nuc (Fig. 1b). In cell-based assays, GS-5734 is active against a broad range of filoviruses including Marburg virus and several variants of EBOV (Fig. 1c). GS-5734 inhibits EBOV replication in multiple relevant human cell types including primary macrophages and human endothelial cells with half-maximum effective concentration (EC_{50}) values of 0.06 to 0.14 μM (Table 1). As expected, the parent Nuc was less active, with EC_{50} values of 0.77 to >20 μM. Treatment with GS-5734 of liver Huh-7 cells infected with the EBOV Makona variant, isolated during the West African outbreak, resulted in profound dose-dependent reductions in viral RNA production and infectious virus yield (Extended Data Fig. 2). GS-5734 and Nuc inhibited replication of other human RNA viral pathogens including
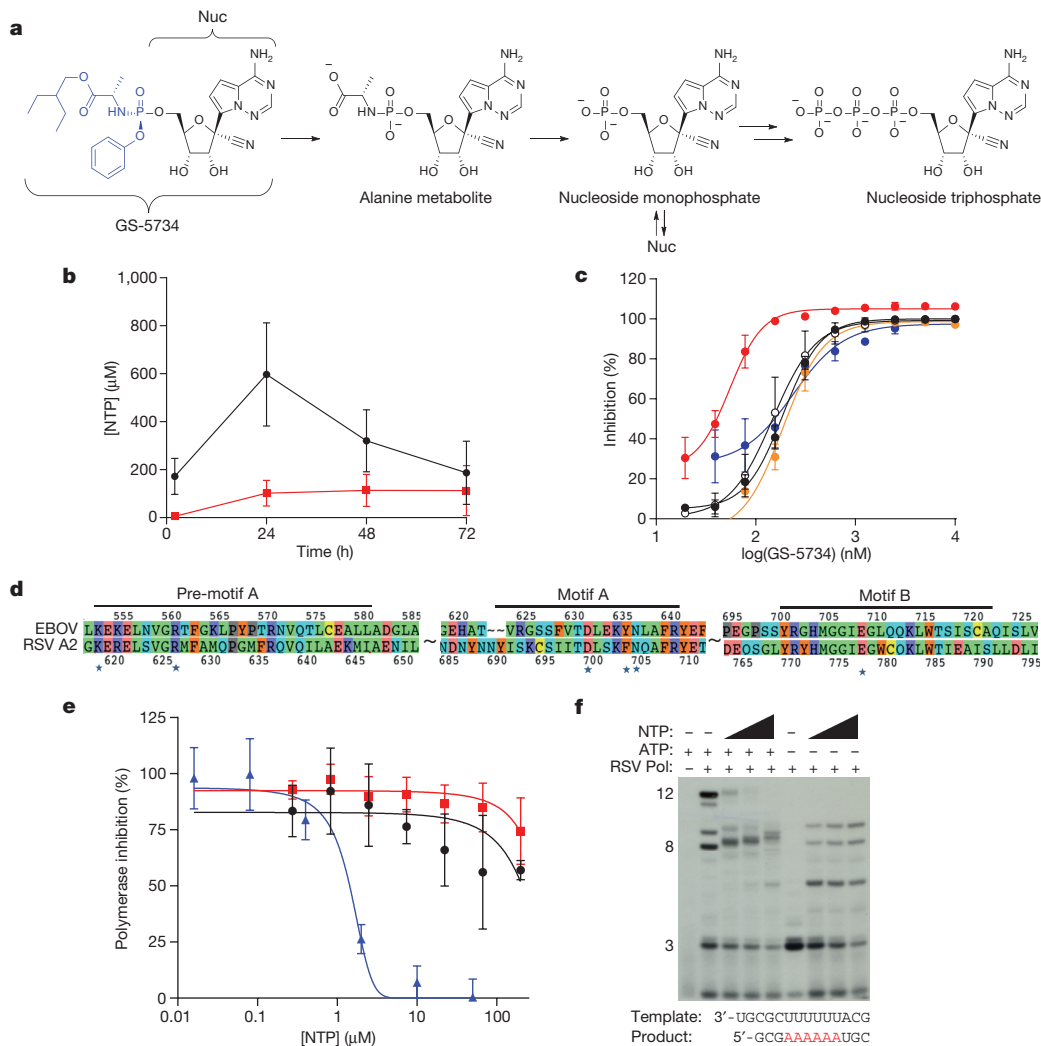
Figure 1 | Metabolism and mechanism of antiviral activity of GS-5734.
a, Chemical structures of GS-5734 and metabolic conversion to NTP.
b, NTP formation in human monocyte-derived macrophages following
72-h incubation with 1 μM GS-5734 (black) or Nuc (red); mean ± s.d.,
from 3 donors. **c**, Antiviral activity of GS-5734 in HeLa cells against EBOV
Makona (black symbols), EBOV Kikwit (open symbols), Marburg (red),
Bundibugyo (orange), Sudan (blue) viruses; mean ± s.d. from triplicates.

d, Amino acid sequence homology of EBOV and RSV strain A2 RdRp
active site. Asterisks indicate residues predicted to contact NTP.
e, Inhibition of RSV RdRp (blue), but not human RNA Pol II (black)
or mitochondrial RNA (red) polymerases by NTP; mean ± s.d., $n = 3$
biological replicates. **f**, NTP-induced RNA chain termination in RSV RdRp
primer-extension assay. For gel source data, see Supplementary Fig. 1.

respiratory syncytial virus (RSV), Junín virus, Lassa fever virus, and
Middle East respiratory syndrome virus, but was inactive against alpha-
viruses or retroviruses (Table 1). Previous studies have reported activity
of Nuc against flaviviruses, parainfluenza virus type 3, and severe acute
respiratory syndrome associated coronavirus, but little or no activity
against West Nile, influenza A, or Coxsackie A viruses[19,21]. The antiviral
activity of GS-5734 was selective, as demonstrated by low cytotoxicity in a
wide range of human primary cells and cell lines (Extended Data Table 1).

Isolation and expression of EBOV RdRp has been elusive, but
computational analysis of the catalytic palm subdomain demonstrated
high sequence and structure homology with RSV RdRp[22] (Fig. 1d,
Extended Data Fig. 3). Consistent with the proposed mechanism of
action, NTP inhibited RSV RdRp-catalysed RNA synthesis (Fig. 1e) by
incorporating into the nascent viral RNA transcript and causing its pre-
mature termination (Fig. 1f). In contrast, NTP did not inhibit human
RNA polymerases (Fig. 1e). These data suggest that GS-5734 selectively
inhibits EBOV replication by targeting its RdRp and inhibiting viral
RNA synthesis following efficient intracellular conversion to NTP.

Rodent models were not suitable for GS-5734 *in vivo* efficacy eval-
uations because high serum esterase activity, present in many rodent
species, degrades the GS-5734 promoiety and adversely impacts its

pharmacokinetic profile[23]. Like humans, rhesus monkeys do not
express high levels of serum esterase; rhesus lymphoid cells efficiently
activated GS-5734 *in vitro*, although NTP levels were reduced relative
to human cells (Extended Data Fig. 1b). In rhesus monkeys, intramus-
cular inoculation with clinically derived wild-type EBOV produces a
fulminant lethal disease with pathophysiological responses that closely
resemble human EVD cases[24,25], and nonhuman primates (NHP) are
considered the most relevant EVD models well-suited for evaluating
the efficacy of antiviral interventions when trials in infected humans
are not feasible.

GS-5734 pharmacokinetics, metabolism, and distribution were
examined in NHPs. Upon intravenous administration of a 10 mg kg^{-1}
dose in rhesus monkeys, GS-5734 exhibited a short plasma half-life
($t_{1/2} = 0.39$ h) with fast systemic elimination followed by the sequential
appearance of transient systemic levels of the key intracellular inter-
mediate alanine metabolite and more persistent levels of Nuc (Fig. 2a).
GS-5734 rapidly distributed into peripheral blood mononuclear cells
(PBMCs), and efficient conversion to NTP was apparent within 2 h
of dose administration. In PBMCs, NTP represents the predominant
metabolite and was persistent with a $t_{1/2}$ of 14 h and levels required
for >50% virus inhibition for 24 h (Fig. 2a, Extended Data Fig. 1c).

Table 1 | Antiviral activity of GS-5734 and Nuc

	Antiviral activity; EC_{50}/EC_{90} (μM)	
	GS-5734	Nuc
EBOV		
Primary macrophages*	0.086/0.18	>20/>20
HeLa cells†	0.14/0.41	>20/>20
HFF-1*	0.13/0.26	>20/>20
HMVEC-TERT cells†	0.06/0.22	0.77/3.12
Huh-7 cells†	0.07/0.22	1.49/6.04
Other human RNA viruses		
RSV‡	0.019/0.051	0.75/2.84
JUNV§	0.47/1.33	
LASV§	1.48/2.80	
MERS§	0.34/4.24	
CHIV§	>20/>20	
VEEV§	>20/>20	
HIV-1§	>20/>20	

Half-maximum cytotoxic concentration (CC_{50}) values for all compounds in primary human cells and human cell lines were greater than the highest concentration tested (>20 μM).
*Mean values from duplicated titrations conducted in differentiated macrophages or HFF-1 cells in a single experiment ($n = 1$). Cells were infected with EBOV (Makona) for antiviral activity determination.
†Mean values from quadruplicate (HMVEC-TERT) or duplicate (Huh-7) titrations generated from two experiments ($n = 2$) or from multiple experiments ($n = 6$) for HeLa cells. Cells were infected with a replication-competent reporter virus (EBOV–GFP) or wild-type EBOV strain Zaire (HeLa) for antiviral activity determination.
‡Mean values from two (GS-5734) or four (Nuc) independent experiments with each drug dilution tested in triplicate against the respiratory syncytial virus (RSV).
§Mean values from duplicate titrations with each drug concentration tested in quadruplicate from a single experiment ($n = 1$).
JUNV, Junín virus; LASV, Lassa fever virus; MERS, Middle East respiratory syndrome coronavirus; CHIV, Chikungunya virus, VEEV, Venezuelan equine encephalitis virus; HIV-1, human immunodeficiency virus type 1.

In cynomolgus monkeys, intravenous administration of a 10 mg kg^{-1} dose of [^{14}C]GS-5734 demonstrated that the drug-derived material distributed to testes, epididymis, eyes, and brain within 4 h of administration (Fig. 2b). Levels in the brain at 4 h were low relative to other tissues, 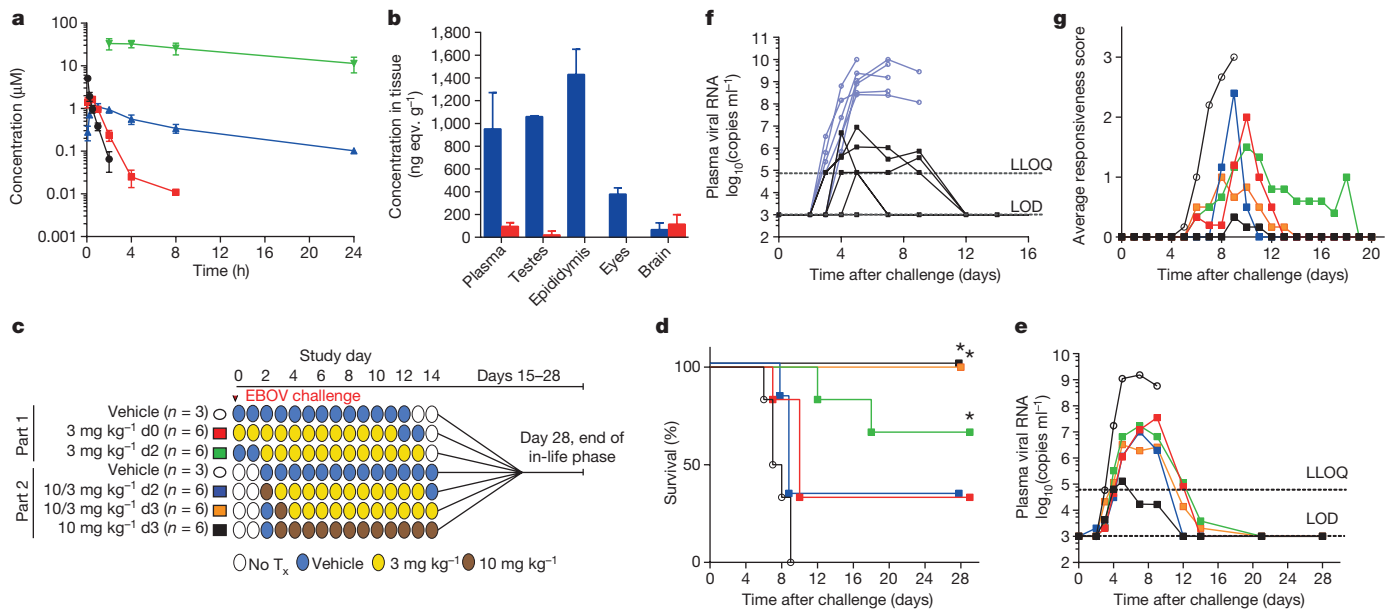but remained detectable above the drug plasma levels 168 h after dose administration. Taken together, the pharmacokinetic analysis indicates that once-daily dosing of GS-5734 provides sustained intracellular NTP levels and efficiently delivers drug metabolites to sanctuary sites where virus may persist.

To evaluate the *in vivo* efficacy of GS-5734, we conducted a sequential two-part adaptive design study in EBOV-infected rhesus monkeys (Fig. 2c). In part 1, animals intramuscularly inoculated with EBOV were administered a 12-day treatment of vehicle ($n = 3$) or 3 mg kg^{-1} GS-5734 beginning on day 0 (d0; 30–90 min following virus challenge) or day 2 (d2) ($n = 6$ per treatment group). Regardless of the time of initiation, GS-5734 treatment conferred an antiviral effect by reducing systemic viraemia relative to vehicle and an improved survival of 33% (2 out of 6) in the 3 mg kg^{-1} d0 group and 66% (4 out of 6) in the 3 mg kg^{-1} d2 group (Fig. 2d, e, Extended Data Fig. 4, Extended Data Tables 2, 3); however, mortalities observed in both treatment groups suggested that drug exposure at 3 mg kg^{-1} was suboptimal. In part 2 of the efficacy study, GS-5734 was administered once at a loading dose of 10 mg kg^{-1} followed by once-daily 3 mg kg^{-1} doses beginning either 2 days (10/3 mg kg^{-1} d2) or 3 days (10/3 mg kg^{-1} d3) after virus exposure, or 10 mg kg^{-1} doses were administered beginning 3 days after virus exposure (10 mg kg^{-1} d3; $n = 6$ per group). All 12 animals in which GS-5734 treatments were initiated 3 days after virus exposure survived to the end of the in-life phase (Fig. 2d). However, the antiviral effects were consistently greater in animals administered repeated 10 mg kg^{-1} GS-5734 doses (Fig. 2e, f, Extended Data Fig. 4, Extended Data Tables 2, 3). On day 4, plasma viral RNA was significantly decreased ($P < 0.05$), with geometric means reduced by ≥ 1.7 log$_{10}$ in all GS-5734-treated groups compared with combined vehicle-treated groups (Fig. 2e, f, Extended Data Table 3), and on days 5 and 7, when the geometric mean viral RNA concentration of the vehicle group exceeded 10^9 copies ml^{-1}, viral RNA was detected at levels less than the lower limit of quantitation (8×10^4 RNA copies ml^{-1}) in 4 of 6 animals in the 10 mg kg^{-1} d3 group. Deep sequencing analysis of the EBOV RdRp (*L*) gene from all plasma samples positive for viral RNA showed no evidence of genotypic changes potentially associated with the emergence of GS-5734-resistant

Figure 2 | GS-5734 pharmacokinetics and post-exposure protection against EBOV in rhesus monkeys. a, Pharmacokinetics following intravenous administration of 10 mg kg^{-1} GS-5734 dose in healthy rhesus macaques (mean ± s.d., $n = 3$). Plasma GS-5734 (black), alanine metabolite (red), and Nuc (blue); NTP in PBMCs (green). **b**, Tissue distribution of [^{14}C]GS-5734 and metabolites at 4 h (blue) and 168 h (red) following intravenous 10 mg kg^{-1} GS-5734 dose in healthy cynomolgus macaques (mean ± s.d., $n = 3$). **c**, Experimental design for GS-5734 efficacy evaluations in rhesus monkeys. No T$_x$, no treatment. **d**, Kaplan–Meier survival curves. *$P < 0.05$ for treatment versus vehicle groups assessed by log-rank analysis using Dunnett–Hsu procedure to adjust for multiple comparisons. **e**, Group geometric mean of plasma viral RNA concentrations; LLOQ, lower limit of quantitation; LOD, limit of detection. **f**, Individual plasma viral RNA in vehicle (blue) or 10 mg kg^{-1} GS-5734 (black) groups. **g**, Group average clinical disease score. **d**, **e**, **g**, Black (open symbols), vehicle; red, 3 mg kg^{-1} d0; green, 3 mg kg^{-1} d2; blue, 10/3 mg kg^{-1} d2; orange, 10/3 mg kg^{-1} d3; black (closed symbols), 10 mg kg^{-1} d3; $n = 6$ animals per group. Error bars omitted for clarity (**e**, **g**); x axes truncated to emphasize acute disease phase (**f**, **g**).
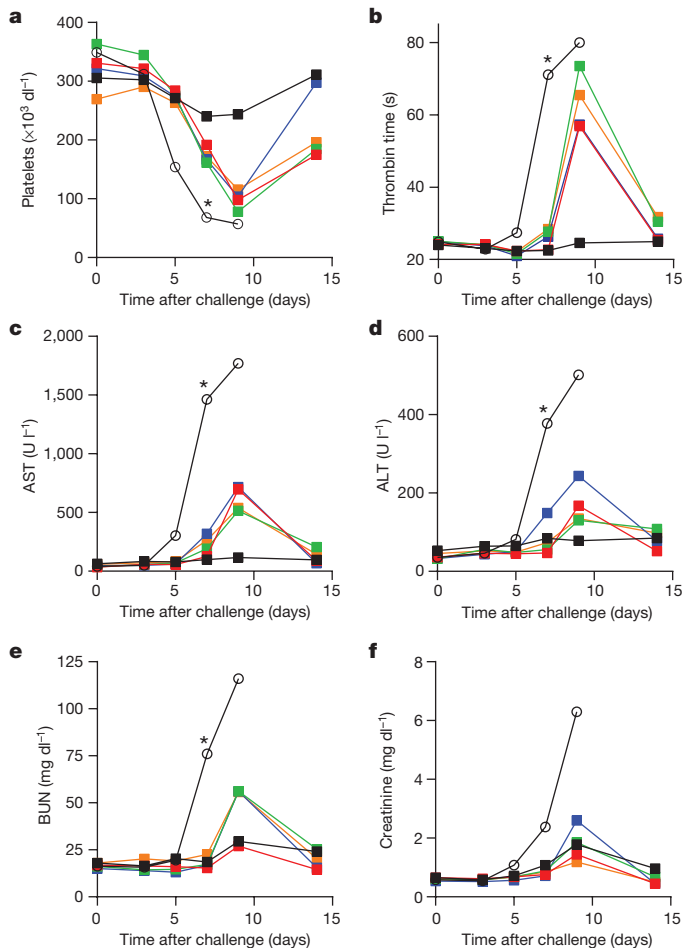
Figure 3 | Amelioration of EVD clinical pathology by GS-5734 in rhesus monkeys. a–f, Group mean ($n = 6$ per group) values of platelets (**a**), thrombin time (**b**), aspartate aminotransferase (AST, **c**), alanine aminotransferase (ALT, **d**), blood urea nitrogen (BUN, **e**), and creatinine (**f**). Black (open symbols), vehicle; red, 3 mg kg⁻¹ d0; green, 3 mg kg⁻¹ d2; blue, 10/3 mg kg⁻¹ d2; orange, 10/3 mg kg⁻¹ d3; black (closed symbols), 10 mg kg⁻¹ d3. Error bars omitted for clarity; x axes truncated at day 15. $*P < 0.05$ for comparison of mean change from day 0 of vehicle and 10 mg kg⁻¹ d3 groups at day 7 using Wilcoxon rank-sum test without adjustment for multiple comparisons.

EBOV variants (Extended Data Table 5). The 10 mg kg⁻¹ d3 GS-5734 regimen was associated with amelioration of EVD-related clinical disease signs (Fig. 2g, Extended Data Fig. 4) and markers of coagulopathy and end-organ pathophysiology (Fig. 3a–f, Extended Data Table 4, Extended Data Fig. 5). Although greater survival was observed in the 10/3 mg kg⁻¹ d3 group than the 10/3 mg kg⁻¹ d2 group, survival and viral RNA load were not statistically distinguishable (Fig. 2d, e) and probably represent natural endpoint variation associated with suboptimal therapeutic effect.

In summary, GS-5734 is a potent and selective inhibitor of EBOV in multiple relevant permissive cell types. In healthy NHPs, intravenous administration of GS-5734 resulted in rapid accumulation and persistence of intracellular NTP. In an NHP model of fatal EVD, pronounced antiviral effects, amelioration of EVD signs, and significant survival benefit was achieved despite treatment initiation on day 3, a time when systemic viral RNA was detectable. These results represent the first case of substantive post-exposure protection against EVD by a small-molecule antiviral compound in NHPs. Intravenous GS-5734 is currently being evaluated in multiple-dose studies in healthy human volunteers to assess clinical safety and pharmacokinetics, and help determine whether GS-5734 may provide therapeutic benefit in acute

or recrudescent cases of EVD, or in survivors with prolonged virus shedding and/or chronic clinical sequelae. The broad-spectrum antiviral activity of GS-5734 and its amenability to large-scale production warrants further assessment of its therapeutic potential against other human viral pathogens for which no treatment is available.

Online Content Methods, along with any additional Extended Data display items and Source Data, are available in the online version of the paper; references unique to these sections appear only in the online paper.

1. World Health Organization. *Ebola Situation Report - 3 February 2016.* http://apps.who.int/ebola/current-situation/ebola-situation-report-3-february-2016 (2016).
2. Nanyonga, M., Saidu, J., Ramsay, A., Shindo, N. & Bausch, D. G. Sequelae of Ebola virus disease, Kenema District, Sierra Leone. *Clin. Infect. Dis.* **62,** 125–126 (2016).
3. Varkey, J. B. *et al.* Persistence of Ebola virus in ocular fluid during convalescence. *N. Engl. J. Med.* **372,** 2423–2427 (2015).
4. Mate, S. E. *et al.* Molecular evidence of sexual transmission of Ebola virus. *N. Engl. J. Med.* **373,** 2448–2454 (2015).
5. Deen, G. F. *et al.* Ebola RNA persistence in semen of Ebola virus disease survivors — preliminary report. *N. Engl. J. Med.* http://dx.doi.org/10.1056/NEJMoa1511410 (2015).
6. Kuhn, J. H. *Filoviruses: A Compendium of 40 Years of Epidemiological, Clinical, and Laboratory Studies* (SpringWien, 2008).
7. Kupferschmidt, K. & Cohen, J. Infectious diseases. Ebola drug trials lurch ahead. *Science* **347,** 701–702 (2015).
8. Smither, S. J. *et al.* Post-exposure efficacy of oral T-705 (Favipiravir) against inhalational Ebola virus infection in a mouse model. *Antiviral Res.* **104,** 153–155 (2014).
9. Oestereich, L. *et al.* Successful treatment of advanced Ebola virus infection with T-705 (favipiravir) in a small animal model. *Antiviral Res.* **105,** 17–21 (2014).
10. McMullan, L. K. *et al.* The lipid moiety of brincidofovir is required for *in vitro* antiviral activity against Ebola virus. *Antiviral Res.* **125,** 71–78 (2016).
11. Sissoko, D. *et al.* Favipiravir in patients with Ebola virus disease: early results of the JIKI trial in Guinea. *Conference of Retroviruses and Opportunistic Infections* abstr. 103-ALB (Seattle, 2015).
12. Chimerix. *Brincidofovir Will Not Be Considered in Further Clinical Trials in Ebola Virus Disease.* http://ir.chimerix.com/releasedetail.cfm?ReleaseID=893927 (2015).
13. Warren, T. K. *et al.* Protection against filovirus diseases by a novel broad-spectrum nucleoside analogue BCX4430. *Nature* **508,** 402–405 (2014).
14. BioCryst Pharmaceuticals. *BioCryst Announces Study Results for BCX4430 in a Non-Human Primate Model of Ebola Virus Infection.* http://investor.shareholder.com/biocryst/releasedetail.cfm?ReleaseID=888802 (2014).
15. Thi, E. P. *et al.* Lipid nanoparticle siRNA treatment of Ebola-virus-Makona-infected nonhuman primates. *Nature* **521,** 362–365 (2015).
16. Qiu, X. *et al.* Reversion of advanced Ebola virus disease in nonhuman primates with ZMapp. *Nature* **514,** 47–53 (2014).
17. Olinger, G. G., Jr *et al.* Delayed treatment of Ebola virus infection with plant-derived monoclonal antibodies provides protection in rhesus macaques. *Proc. Natl Acad. Sci. USA* **109,** 18030–18035 (2012).
18. Tekmira Pharmaceuticals Corporation. *Tekmira Provides Update on TKM-Ebola-Guinea.* http://www.sec.gov/Archives/edgar/data/1447028/000117184315003522/newsrelease.htm (2015).
19. Cho, A. *et al.* Synthesis and antiviral activity of a series of 1'-substituted 4-aza-7,9-dideazaadenosine C-nucleosides. *Bioorg. Med. Chem. Lett.* **22,** 2705–2707 (2012).
20. Murakami, E. *et al.* The mechanism of action of β-D-2'-deoxy-2'-fluoro-2'-C-methylcytidine involves a second metabolic pathway leading to β-D-2'-deoxy-2'-fluoro-2'-C-methyluridine 5'-triphosphate, a potent inhibitor of the hepatitis C virus RNA-dependent RNA polymerase. *Antimicrob. Agents Chemother.* **52,** 458–464 (2008).
21. Mackman, R. L., Parrish, J. P., Ray, A. S. & Theodore, D. A. Methods and compounds for treating respiratory syncytial virus infections. US Patent 2011045102. (2011).
22. Jácome, R., Becerra, A., Ponce de Leon, S. & Lazcano, A. Structural analysis of monomeric RNA-dependent polymerases: Evolutionary and therapeutic implications. *PLoS ONE* **10,** e0139001 (2015).
23. Bahar, F. G., Ohura, K., Ogihara, T. & Imai, T. Species difference of esterase expression and hydrolase activity in plasma. *J. Pharm. Sci.* **101,** 3979–3988 (2012).
24. Hunt, L. *et al.* Clinical presentation, biochemical, and haematological parameters and their association with outcome in patients with Ebola virus disease: an observational cohort study. *Lancet Infect. Dis.* **15,** 1292–1299 (2015).
25. Martins, K. *et al.* Characterization of clinical and immunological parameters during Ebola virus infection of rhesus macaques. *Viral Immunol.* **28,** 32–41 (2015).

METHODS

Data reporting. No statistical methods were used to predetermine sample size for biochemical or cell-based assays, or for pharmacokinetic studies. Investigators were not blinded to outcome assessment during these investigations. For GS-5734 efficacy assessments in nonhuman primates, statistical power analysis was used to predetermine sample size, and subjects were randomly assigned to experimental group, stratified by sex and balanced by body weight. Study personnel responsible for assessing animal health (including euthanasia assessment) and administering treatments were experimentally blinded to group assignment of animals and outcome.

Small molecules. GS-5734, Nuc, and NTP were synthesized at Gilead Sciences, Inc., and chemical identity and sample purity were established using NMR, HRMS, and HPLC analysis (Supplementary Information). The radiolabelled analogue [^{14}C]GS-5734 (specific activity, 58.0 mCi mmol^{-1}) was obtained from Moravek Biochemicals (Brea, California) and was prepared in a similar manner described for GS-5734 using [^{14}C]trimethylsilylcyanide (Supplementary Information). Small molecule X-ray crystallographic coordinates and structure factor files have been deposited in the Cambridge Structural Database (http://www.ccdc.cam.ac.uk/) and accession numbers are supplied in the Supplementary Information.

Viruses. RSV A2 was purchased from Advanced Biotechnologies, Inc. EBOV (Kikwit and Makona variants), Sudan virus (SUDV, Gulu), Marburg virus (MARV, Ci67), Junín virus (JUNV, Romero), Lassa virus (LASV, Josiah), Middle East respiratory syndrome virus (MERS, Jordan N3), Chikungunya virus (CHIV, AF 15561), and Venezuelan equine encephalitis virus (VEEV, SH3) were all prepared and characterized at the United States Army Medical Research Institute for infectious diseases (USAMRIID). EBOV containing a GFP reporter gene (EBOV–GFP), EBOV Makona (Liberia, 2014), and MARV containing a GFP reporter gene (MARV–GFP) were prepared and characterized at the Centers for Disease Control and Prevention[26,27].

Cells. HEp-2 (CCL-23), PC-3 (CCL-1435), HeLa (CCL-2), U2OS (HTB-96), Vero (CCL-81), HFF-1 (SCRC-1041), and HepG2 (HB-8065) cell lines were purchased from the American Type Culture Collection. Cell lines were not authenticated and were not tested for mycoplasma as part of routine use in assays. HEp-2 cells were cultured in Eagle's Minimum Essential Media (MEM) with GlutaMAX supplemented with 10% fetal bovine serum (FBS) and 100 U ml^{-1} penicillin and streptomycin. PC-3 cells were cultured in Kaighn's F12 media supplemented with 10% FBS and 100 U ml^{-1} penicillin and streptomycin. HeLa, U2OS, and Vero cells were cultured in MEM supplemented with 10% FBS, 1% L-glutamine, 10 mM HEPES, 1% non-essential amino acids, and 1% penicillin/streptomycin. HFF-1 cells were cultured in MEM supplemented with 10% FBS and 0.5 mM sodium pyruvate. HepG2 cells were cultured in Dulbecco's Modified Eagle Medium (DMEM) with GlutaMAX supplemented with 10% FBS, 100 U ml^{-1} penicillin and streptomycin, and 0.1 mM non-essential amino acids. The MT-4 cell line was obtained from the NIH AIDS Research and Reference Reagent Program and cultured in RPMI-1640 medium supplemented with 10% FBS, 100 U ml^{-1} penicillin and streptomycin, and 2 mM L-glutamine. The Huh-7 cell line was obtained from C. M. Rice (Rockefeller University) and cultured in DMEM supplemented with 10% FBS, 100 U ml^{-1} penicillin and streptomycin, and non-essential amino acids.

Primary human hepatocytes were purchased from Invitrogen and cultured in William's Medium E medium containing cell maintenance supplement. Donor profiles were limited to 18- to 65-year-old nonsmokers with limited alcohol consumption. Upon delivery, the cells were allowed to recover for 24 h in complete medium with supplement provided by the vendor at 37 °C. Human PBMCs were isolated from human buffy coats obtained from healthy volunteers (Stanford Medical School Blood Center, Palo Alto, California) and maintained in RPMI-1640 with GlutaMAX supplemented with 10% FBS, 100 U ml^{-1} penicillin and streptomycin. Rhesus fresh whole blood was obtained from Valley Biosystems. PBMCs were isolated from whole blood by Ficoll-Hypaque density gradient centrifugation. Briefly, blood was overlaid on 15 ml Ficoll-Paque (GE Healthcare Bio-Sciences AB), and centrifuged at 500g for 20 min. The top layer containing platelets and plasma was removed, and the middle layer containing PBMCs was transferred to a fresh tube, diluted with Tris buffered saline up to 50 ml, and centrifuged at 500g for 5 min. The supernatant was removed and the cell pellet was resuspended in 5 ml red blood cell lysis buffer (155 mM ammonium chloride, 10 mM potassium bicarbonate, 0.1 mM EDTA, pH 7.5). To generate stimulated PBMCs, freshly isolated quiescent PBMCs were seeded into a T-150 (150 cm^2) tissue culture flask containing fresh medium supplemented with 10 U ml^{-1} of recombinant human interleukin-2 (IL-2) and 1 µg ml^{-1} phytohaemagglutinin-P at a density of 2×10^6 cells ml^{-1} and incubated for 72 h at 37 °C. Human macrophage cultures were isolated from PBMCs that were purified by Ficoll gradient centrifugation from 50 ml of blood from healthy human volunteers. PBMCs were cultured for 7 to 8 days in in RPMI cell culture media supplemented with 10% FBS, 5 to 50 ng ml^{-1} granulocyte-macrophage colony-stimulating

factor and 50 µM β-mercaptoethanol to induce macrophage differentiation. The cryopreserved human primary renal proximal tubule epithelial cells were obtained from LifeLine Cell Technology and isolated from the tissue of human kidney. The cells were cultured at 90% confluency with RenaLife complete medium in a T-75 flask for 3 to 4 days before seeding into 96-well assay plates. Immortalized human microvascular endothelial cells (HMVEC-TERT) were obtained from R. Shao at the Pioneer Valley Life Sciences Institute[28]. HMVEC-TERT cells were cultured in endothelial basal media supplemented with 10% FBS, 5 µg of epithelial growth factor, 0.5 mg hydrocortisone, and gentamycin/amphotericin-B.

Enzymes. RNA POLII was purchased as part of the HeLaScribe Nuclear Extract *in vitro* Transcription System kit from Promega. The recombinant human POLRMT and transcription factors mitochondrial transcription factors A (mtTFA or TFAM) and B2 (mtTFB2 or TFB2M) were purchased from Enzymax. RSV ribonucleoprotein (RNP) complexes were prepared according to a method modified from ref. 29.

Intracellular metabolism studies. The intracellular metabolism of GS-5734 was assessed in different cell types (HMVEC and HeLa cell lines, and primary human and rhesus PBMCs, monocytes and monocyte-derived macrophages) following 2-h pulse or 72-h continuous incubations with 10 µM GS-5734. For comparison, intracellular metabolism during a 72-h incubation with 10 µM of Nuc was completed in human monocyte-derived macrophages. For pulse incubations, monocyte-derived macrophages isolated from rhesus monkeys or humans were incubated for 2 h in compound-containing media followed by removal, washing with 37 °C drug-free media, and incubated for an additional 22 h in media which did not contain GS-5734. Human monocyte-derived macrophages, HeLa and HMVEC were grown to confluence (approximately 0.5, 0.2, and 1.2×10^6 cells per well, respectively) in 500 µl of media in 12-well tissue culture plates. Monocyte and PBMCs were incubated in suspension (approximately 1×10^6 cells ml^{-1}) in 1 ml of media in micro centrifuge tubes.

For adherent cells (HMVEC, HeLa, and monocyte-derived macrophages), media was removed at select time points from duplicate wells, cells washed twice with 2 ml of ice-cold 0.9% normal saline. For non-adherent cells (monocytes and PBMCs), duplicate incubations were centrifuged at 2,500g for 30 s to remove media. The cell pellets were re-suspended with 500 µl cell culture media (RPMI with 10% FBS) and layered on top of a 500 µl oil layer (Nyosil M25; Nye Lubricants) in a microcentrifuge tube. Samples were then centrifuged at room temperature at 13,000 r.p.m. for 45 s. The media layer was removed and the oil layer was washed twice with 500 µl water. The oil layer was then carefully removed using a Pasteur pipet attached to vacuum. A volume of 0.5 ml of 70% methanol containing 100 nM of the analytical internal standard 2-chloro-adenosine-5′-triphosphate (Sigma-Aldrich) was added to isolated cells. Samples were stored overnight at −20 °C to facilitate extraction, centrifuged at 15,000g for 15 min and then supernatant was transferred to clean tubes for drying in a MiVac Duo concentrator (Genevac). Dried samples were then reconstituted in mobile phase A containing 3 mM ammonium formate (pH 5.0) with 10 mM dimethylhexylamine (DMH) in water for analysis by liquid chromatography coupled to triple quadrupole mass spectrometry (LC-MS/MS).

LC-MS/MS was performed using low-flow ion-pairing chromatography, similar to methods described previously[30]. Briefly, analytes were separated using a 50×2 mm $\times$ 2.5 µm Luna C18(2) HST column (Phenomenex) connected to a LC-20ADXR (Shimadzu) ternary pump system and HTS PAL autosampler (LEAP Technologies). A multi-stage linear gradient from 10% to 50% acetonitrile in a mobile phase containing 3 mM ammonium formate (pH 5.0) with 10 mM dimethylhexylamine over 8 min at a flow rate of 150 µl min^{-1} was used to separate analytes. Detection was performed on an API 4000 (Applied Biosystems) MS/MS operating in positive ion and multiple reaction monitoring modes. Intracellular metabolites alanine metabolite, Nuc, nucleoside monophosphate, nucleoside diphosphate, and nucleoside triphosphate were quantified using 7-point standard curves ranging from 0.274 to 200 pmol (approximately 0.5 to 400 µM) prepared in cell extract from untreated cells. Levels of adenosine nucleotides were also quantified to assure dephosphorylation had not taken place during sample collection and preparation. In order to calculate intracellular concentration of metabolites, the total number of cells per sample were counted using a Countess automated cell counter (Invitrogen).

EBOV Huh-7 and HMVEC antiviral assay. Antiviral assays were conducted in biosafety level 4 containment (BSL-4) at the Centers for Disease Control and Prevention. EBOV antiviral assays were conducted in primary HMVEC-TERT and in Huh-7 cells. Huh-7 cells were not authenticated and were not tested for mycoplasma. Ten concentrations of compound were diluted in fourfold serial dilution increments in media, and 100 µl per well of each dilution was transferred in duplicate (Huh-7) or quadruplicate (HMVEC-TERT) onto 96-well assay plates containing cell monolayers. The plates were transferred to BSL-4 containment, and the appropriate dilution of virus stock was added to test plates containing cells and serially diluted compounds. Each plate included four wells of infected

untreated cells and four wells of uninfected cells that served as 0% and 100% virus inhibition controls, respectively. After the infection, assay plates were incubated for 3 days (Huh-7) or 5 days (HMVEC-TERT) in a tissue culture incubator. Virus replication was measured by direct fluorescence using a Biotek HTSynergy plate reader. For virus yield assays, Huh-7 cells were infected with wild-type EBOV for 1 h at 0.1 plaque-forming units (PFU) per cell. The virus inoculum was removed and replaced with 100 μl per well of media containing the appropriate dilution of compound. At 3 days post-infection, supernatants were collected, and the amount of virus was quantified by endpoint dilution assay. The endpoint dilution assay was conducted by preparing serial dilutions of the assay media and adding these dilutions to fresh Vero cell monolayers in 96-well plates to determine the tissue culture infectious dose that caused 50% cytopathic effects ($TCID_{50}$). To measure levels of viral RNA from infected cells, total RNA was extracted using the MagMAX-96 Total RNA Isolation Kit and quantified using a quantitative reverse transcription polymerase chain reaction (qRT–PCR) assay with primers and probes specific for the EBOV nucleoprotein gene.

EBOV assay in HeLa and HFF-1 cells. Antiviral assays were conducted in BSL-4 at USAMRIID. HeLa or HFF-1 cells were seeded at 2,000 cells per well in 384-well plates. Ten serial dilutions of compound in triplicate were added directly to the cell cultures using the HP D300 digital dispenser (Hewlett Packard) in twofold dilution increments starting at 10 μM at 2 h before infection. The DMSO concentration in each well was normalized to 1% using an HP D300 digital dispenser. The assay plates were transferred to the BSL-4 suite and infected with EBOV Kikwit at a multiplicity of infection of 0.5 PFU per cell for HeLa cells and with EBOV Makona at a multiplicity of infection of 5 PFU per cell for HFF-1 cells. The assay plates were incubated in a tissue culture incubator for 48 h. Infection was terminated by fixing the samples in 10% formalin solution for an additional 48 h before immune-staining, as described in Supplementary Table 1.

EBOV human macrophage infection assay. Antiviral assays were conducted in BSL-4 at USAMRIID. Primary human macrophage cells were seeded in a 96-well plate at 40,000 cells per well. Eight to ten serial dilutions of compound in triplicate were added directly to the cell cultures using an HP D300 digital dispenser in threefold dilution increments 2 h before infection. The concentration of DMSO was normalized to 1% in all wells. The plates were transferred into the BSL-4 suite, and the cells were infected with 1 PFU per cell of EBOV in 100 μl of media and incubated for 1 h. The inoculum was removed, and the media was replaced with fresh media containing diluted compounds. At 48 h post-infection, virus replication was quantified by immuno-staining as described in Supplementary Table 1.

RSV A2 antiviral assay. For antiviral tests, compounds were threefold serially diluted in source plates from which 100 nl of diluted compound was transferred to a 384-well cell culture plate using an Echo acoustic transfer apparatus. HEp-2 cells were added at a density of 5×10^5 cells per ml, then infected by adding RSV A2 at a titer of $1 \times 10^{4.5}$ tissue culture infectious doses ($TCID_{50}$) per ml. Immediately following virus addition, 20 μl of the virus and cells mixture was added to the 384-well cell culture plates using a μFlow liquid dispenser and cultured for 4 days at 37 °C. After incubation, the cells were allowed to equilibrate to 25 °C for 30 min. The RSV-induced cytopathic effect was determined by adding 20 μl of CellTiter-Glo Viability Reagent. After a 10-min incubation at 25 °C, cell viability was determined by measuring luminescence using an Envision plate reader.

High content imaging assay detecting viral infection. Antiviral assays were conducted in 384- or 96-well plates in BSL-4 at USAMRIID using a high-content imaging system to quantify virus antigen production as a measure of virus infection. A 'no virus' control and a '1% DMSO' control were included to determine the 0% and 100% virus infection, respectively. The primary and secondary antibodies and dyes used for nuclear and cytoplasmic staining are listed in Supplementary Table 1. The primary antibody specific for a particular viral protein was diluted 1,000-fold in blocking buffer (1 × PBS with 3% BSA) and added to each well of the assay plate. The assay plates were incubated for 60 min at room temperature. The primary antibody was removed, and the cells were washed three times with 1 × PBS. The secondary detection antibody was an anti-mouse (or rabbit) IgG conjugated with Dylight488 (Thermo Fisher Scientific, catalogue number 405310). The secondary antibody was diluted 1,000-fold in blocking buffer and was added to each well in the assay plate. Assay plates were incubated for 60 min at room temperature. Nuclei were stained using Draq5 (Biostatus) or 33342 Hoechst (ThermoFisher Scientific) for Vero and HFF-1 cell lines. Both dyes were diluted in 1× PBS. The cytoplasm of HFF-1 (EBOV assay) and Vero E6 (MERS assay) cells were counter-stained with CellMask Deep Red (Thermo Fisher Scientific). Cell images were acquired using a Perkin Elmer Opera confocal plate reader (Perkin Elmer) using a ×10 air objective to collect five images per well. Virus-specific antigen was quantified by measuring fluorescence emission at a 488 nm wavelength and the stained nuclei were quantified by measuring fluorescence emission at a 640 nm wavelength. Acquired images were analysed using Harmony and Acapella PE software. The Draq5 signal was used to generate a nuclei mask to define each

nuclei in the image for quantification of cell number. The CellMask Deep Red dye was used to demarcate the Vero and HFF-1 cell borders for cell-number quantitation. The viral-antigen signal was compartmentalized within the cell mask. Cells that exhibited antigen signal higher than the selected threshold were counted as positive for viral infection. The ratio of virus-positive cells to total number of analysed cells was used to determine the percentage of infection for each well on the assay plates. The effect of compounds on the viral infection was assessed as percentage of inhibition of infection in comparison to control wells. The resultant cell number and percentage of infection were normalized for each assay plate. Analysis of dose–response curve was performed using GeneData Screener software applying Levenberg–Marquardt algorithm for curve-fitting strategy. The curve-fitting process, including individual data point exclusion, was pre-specified by default software settings. R^2 value quantified goodness of fit and fitting strategy was considered acceptable at $R^2 > 0.8$.

Virus assays. All virus infections were quantified by immuno-staining using antibodies that recognized the relevant viral glycoproteins, as described in Supplementary Table 1.

Marburg virus assay. HeLa cells were seeded at 2,000 cells per well in a 384-well plate, and compounds were added to the assay plates. Assay plates were transferred to the BSL-4 suite and infected with 1 PFU per cell MARV, which resulted in 50% to 70% of the cells expressing virus antigen in a 48-h period.

Sudan virus assay. HeLa cells were seeded at 2,000 cells per well in a 384-well plate, and compounds were added to the assay plates. Assay plates were transferred to the BSL-4 suite and infected with 0.08 PFU SUDV per cell, which resulted in 50% to 70% of the cells expressing virus antigen in a 48-h period.

Junín virus assay. HeLa cells were seeded at 2,000 cells per well in a 384-well plate, and compounds were added to the assay plates. Assay plates were transferred to the BSL-4 suite and infected with 0.3 PFU per cell JUNV, which resulted in ~50% of the cells expressing virus antigen in a 48-h period.

Lassa fever virus assay. HeLa cells were seeded at 2,000 cells per well in a 384-well plate, and compounds were added to the assay plates. Assay plates were transferred to the BSL-4 suite and infected with 0.1 PFU per cell LASV, which resulted in >60% of the cells expressing virus antigen in a 48-h period.

Middle East respiratory syndrome virus assay. African green monkey (*Chlorocebus* sp.) kidney epithelial cells (Vero E6) were seeded at 4,000 cells per well in a 384-well plate, and compounds were added to the assay plates. Assay plates were transferred to the BSL-4 suite and infected with 0.5 PFU per cell of MERS virus, which resulted in >70% of the cells expressing virus antigen in a 48-h period.

Chikungunya virus assay. U2OS cells were seeded at 3,000 cells per well in a 384-well plate, and compounds were added to the assay plates. Assay plates were transferred to the BSL-4 suite and infected with 0.5 PFU per cell of CHIK, which resulted in >80% of the cells expressing virus antigen in a 48-h period.

Venezuelan equine encephalitis virus assay. HeLa cells were seeded at 4,000 cells per well in a 384-well plate, and compounds were added to the assay plates. Assay plates were transferred to the BSL-4 suite and infected with 0.1 PFU per cell VEEV, which resulted in >60% of the cells expressing virus antigen in a 20-h period.

Cytotoxicity assays. HEp-2 (1.5×10^3 cells per well) and MT-4 (2×10^3 cells per well) cells were plated in 384-well plates and incubated with the appropriate medium containing threefold serially diluted compound ranging from 15 nM to 100,000 nM. PC-3 (2.5×10^3 cells per well), HepG2 cells (4×10^3 cells per well), hepatocytes (1×10^6 cells per well), quiescent PBMCs (1×10^6 cells per well), stimulated PBMCs (2×10^5 cells per well), and RPTEC cells (1×10^3 cells per well) were plated in 96-well plates and incubated with the appropriate medium containing threefold serially diluted compound ranging from 15 nM to 100,000 nM. Cells were cultured for 4–5 days at 37 °C. Following the incubation, the cells were allowed to equilibrate to 25 °C, and cell viability was determined by adding Cell-Titer Glo viability reagent. The mixture was incubated for 10 min, and the luminescence signal was quantified using an Envision plate reader. Cell lines were not authenticated and were not tested for mycoplasma as part of routine use in cytotoxicity assays.

In vitro **RSV RNA synthesis assay.** RNA synthesis by the RSV polymerase was reconstituted *in vitro* using purified RSV L/P complexes and an RNA oligonucleotide template (Dharmacon), representing nucleotides 1–14 of the RSV leader promoter[31–33] (3′-UGCGCUUUUUUACG-5′). RNA synthesis reactions were performed as described previously, except that the reaction mixture contained 250 μM guanosine triphosphate (GTP), 10 μM uridine triphosphate (UTP), 10 μM cytidine triphosphate (CTP), supplemented with 10 μCi [α-^{32}P]CTP, and either included 10 μM adenosine triphosphate (ATP) or no ATP. Under these conditions, the polymerase is able to initiate synthesis from the position 3 site of the promoter, but not the position 1 site. The NTP metabolite of GS-5734 was serially diluted in DMSO and included in each reaction mixture at concentrations of 10, 30, or 100 μM as specified in Fig. 1f. RNA products were analysed by electrophoresis on a 25% polyacrylamide gel, containing 7 M urea, in Tris–taurine–EDTA buffer, and radiolabelled RNA products were detected by autoradiography.

RSV A2 polymerase inhibition assay. Transcription reactions contained 25 μg of crude RSV RNP complexes in 30 μL of reaction buffer (50 mM Tris-acetate (pH 8.0), 120 mM potassium acetate, 5% glycerol, 4.5 mM MgCl$_2$, 3 mM DTT, 2 mM EGTA, 50 μg ml^{-1} BSA, 2.5 U RNasin, 20 μM ATP, 100 μM GTP, 100 μM UTP, 100 μM CTP, and 1.5 μCi [α-^{32}P]ATP (3,000 Ci mmol^{-1})). The radiolabelled nucleotide used in the transcription assay was selected to match the nucleotide analogue being evaluated for inhibition of RSV RNP transcription.

To determine whether nucleotide analogues inhibited RSV RNP transcription, compounds were added using a six-step serial dilution in fivefold increments. After a 90-min incubation at 30 °C, the RNP reactions were stopped with 350 μl of Qiagen RLT lysis buffer, and the RNA was purified using a Qiagen RNeasy 96 kit. Purified RNA was denatured in RNA sample loading buffer at 65 °C for 10 min and run on a 1.2% agarose/MOPS gel containing 2 M formaldehyde. The agarose gel was dried, exposed to a Storm phosphorimaging screen, and developed using a Storm phosphorimager.

Inhibition of human RNA polymerase II. For a 25 μl reaction mixture, 7.5 μl 1 × transcription buffer (20 mM HEPES (pH 7.2–7.5), 100 mM KCl, 0.2 mM EDTA, 0.5 mM DTT, 20% glycerol), 3 mM MgCl$_2$, 100 ng CMV positive or negative control DNA, and a mixture of ATP, GTP, CTP and UTP was pre-incubated with various concentrations (0–500 μM) of the inhibitor at 30 °C for 5 min. The mixture contained 5–25 μM (equal to K_m) of the competing ^{33}P-labelled ATP and 400 μM of GTP, UTP, and CTP. The reaction was started by addition of 3.5 μl of HeLa and extract. After 1 h of incubation at 30 °C, the polymerase reaction was stopped by addition of 10.6 μl proteinase K mixture that contained final concentrations of 2.5 μg μl^{-1} proteinase K, 5% SDS, and 25 mM EDTA. After incubation at 37 °C for 3–12 h, 10 μl of the reaction mixture was mixed with 10 μl of the loading dye (98% formamide, 0.1% xylene cyanol and 0.1% bromophenol blue), heated at 75 °C for 5 min, and loaded onto a 6% polyacrylamide gel (8 M urea). The gel was dried for 45 min at 70 °C and exposed to a phosphorimager screen. The full length product, 363 nucleotide runoff RNA, was quantified using a Typhoon Trio Imager and Image Quant TL Software.

Inhibition of human mitochondrial RNA polymerase. Twenty nanomolar POLRMT was incubated with 20 nM template plasmid (pUC18-LSP) containing POLRMT light-strand promoter region and mitochondrial (mt) transcription factors TFA (100 nM) and mtTFB2 (20 nM) in buffer containing 10 mM HEPES (pH 7.5), 20 mM NaCl, 10 mM DTT, 0.1 mg ml^{-1} BSA, and 10 mM MgCl$_2$[34]. The reaction mixture was pre-incubated to 32 °C, and the reactions were initiated by addition of 2.5 μM of each of the natural NTPs and 1.5 μCi of [^{32}P]GTP. After incubation for 30 min at 32 °C, reactions were spotted on DE81 paper and quantified.

Molecular modelling. A homology model of RSV A2 and EBOV polymerases were built using the HIV reverse transcriptase X-ray crystal structure (PDB:1RTD). Schrödinger Release 2015-1: Prime, version 3.9 (Schrödinger, LLC), default settings with subsequent rigid body minimization and side-chain optimization. Loop insertions not in 1RTD of greater than 10 amino acids were not built.

qRT–PCR for *in vivo* studies. For quantitative assessment of viral RNA non-human primate plasma samples, whole blood was collected using a K3 EDTA Greiner Vacuette tube (or equivalent) and sample centrifuged at 2500 (± 200) relative centrifugal force for 10 ± 2 min. To inactivate virus, plasma was treated with 3 parts (300 μl) TriReagent LS and samples were transferred to frozen storage (−60 °C to −90 °C), until removal for RNA extraction. Carrier RNA and QuantiFast High Concentration Internal Control (Qiagen) were spiked into the sample before extraction, conducted according to manufacturer's instructions. The viral RNA was eluted in AVE buffer. Each extracted RNA sample was tested with the QuantiFast Internal Control RT–PCR RNA Assay (Qiagen) to evaluate the yield of the spiked-in QuantiFast High Concentration Internal Control. If the internal control amplified within manufacturer-designated ranges, further quantitative analysis of the viral target was performed. RT–PCR was conducted using an ABI 7500 Fast Dx using primers specific to EBOV glycoprotein. Samples were run in triplicate using a 5 μl template volume. For quantitative assessments, the average of the triplicate genomic equivalents (GE) per reaction were determined and multiplied by 800 to obtain GE ml^{-1} plasma. Standard curves were generated using synthetic RNA. The limits of quantification for this assay are $8.0 \times 10^4 – 8.0 \times 10^{10}$ GE ml^{-1} of plasma. Acceptance criteria for positive template control (PTC), negative template control (NTC), negative extraction control (NEC), and positive extraction control (PEC) are specified by standard operating procedure. For qualitative assessments, the limit of detection (LOD) was defined as C_t 38.07, based on method validation testing. An animal was considered to have tested positive for detection of EBOV RNA when a minimum of 2 of 3 replicates were designated as 'positive' and PTC, NTC, and NEC controls met specified method-acceptance criteria. A sample was designated as 'positive' when the C_t value was < LOD C_t.

Pharmacokinetic evaluations. Three uninfected male rhesus monkeys (*Macaca mulatta*) were used for the pharmacokinetic study. GS-5734 was formulated in solution at 5 mg ml^{-1} with 12% sulfobutylether-β-cyclodextrin in water,

pH 3.5–4.0, and 2 ml kg^{-1} was administered by slow bolus (approximately 1 min) for a final dose of 10 mg kg^{-1}. Blood samples for plasma and PBMCs were collected from a femoral vein/artery and were taken from each monkey over a 24-h period. Plasma samples were obtained at predose and at 0.083, 0.25, 0.5, 1, 2, 4, 8, and 24 h postdose. PBMC samples were obtained at 2, 4, 8, and 24 h. Blood samples for plasma were collected into chilled collection tubes containing sodium fluoride/potassium oxalate as the anticoagulant and were immediately placed on wet ice, followed by centrifugation to obtain plasma. Blood samples for PBMC isolation were collected at room temperature into CPT vacutainer tubes containing sodium heparin for isolation. Plasma and isolated PBMC samples were frozen immediately and stored at ≤60 °C until analysed.

For plasma analysis, an aliquot of 25 μl of each plasma sample was treated with 100 μl of 90% methanol and acetonitrile mixture (1:1, v:v) and 10% water with 20 nM 5-(2-aminopropyl)indole as an internal standard. Then, 100 μl of samples were filtered through an Agilent Captiva 96 well 0.2 μm filter plate. Filtered samples were dried down completely for approximately 20 min and reconstituted with 1% acetonitrile and 99% water with 0.01% formic acid. An aliquot of 10 μl was injected for LC-MS/MS using a HTC Pal autosampler. Analytes were separated on a Phenomenex Synergi Hydro-RP 30A column (75 × 2.0 mM, 4.0 μm) using a Waters Acquity ultra performance LC (Waters Corporation, Milford, MA, USA), a flow rate of 0.26 ml min^{-1}, and a gradient from Mobile phase A containing 0.2% formic acid in 99% water and 1% acetonitrile to mobile phase B containing 0.2% formic acid in 95% acetonitrile and 5% water over 4.5 min. For MS/MS analysis, we used a Waters Xevo TQ-S in positive multiple reaction monitoring mode using an electrospray probe. Plasma concentrations of GS-734, alanine metabolite and Nuc were determined using an 8-point calibration curve spanning a concentration range of over three orders of magnitude. Quality control samples were run at the beginning and end of the run to ensure accuracy and precision within 20%. Intracellular metabolites in PBMCs were quantified by LC-MS/MS as described above for *in vitro* activation studies.

Radiolabelled tissue distribution. Six cynomolgus monkeys (*Macaca fascicularis*) were administered a single dose of [^{14}C]GS-5734 at 10 mg kg^{-1} (25 μCi kg^{-1}) by intravenous administration (slow bolus). Tissues were collected from three animals at 4 and 168 h postdose. The tissues were excised, rinsed with saline, blotted dry, weighed, and placed on wet ice. Tissues (testes, epididymis, eyes and brain; following homogenization) and plasma were analysed by liquid scintillation counting. Concentrations were converted to ng equivalents of GS-5734 per gram of sample.

***In vivo* efficacy.** Rhesus monkeys (*Macaca mulatta*) were challenged on day 0 by intramuscular injection with a target dose of 1,000 PFU of EBOV Kikwit (Ebola virus H. sapiens-tc/COD/1995/Kikwit), which was derived from a clinical specimen obtained during an outbreak occurring in the Democratic Republic of the Congo (formerly Zaire) in 1995. Challenge virus was propagated from the clinical specimen using cultured cells (Vero or Vero E6) for a total of four passages. Animals (3–6 years old) were randomly assigned to experimental treatment groups, stratified by sex (with equal number of males and females per group) and balanced by body weight, using SAS statistical software. Study personnel responsible for assessing animal health (including euthanasia assessment) and administering treatments were experimentally blinded to group assignment of animals. The primary endpoint for efficacy studies was survival to day 28 following virus challenge. GS-5734 was formulated at Gilead Sciences in water with 12% sulfobutylether-β-cyclodextrin (SBE-β-CD), pH adjusted to 3.0 using HCl. Formulations were administered to anaesthetized animals by bolus intravenous injection at a rate of approximately 1 min per dose in the right or left saphenous vein. The volume of all vehicle or GS-5734 injections was 2.0 ml kg^{-1} body weight. Animals were anaesthetized using intramuscular injection of a solution containing ketamine (100 mg ml^{-1}) and acepromazine (10 mg ml^{-1}) at 0.1 ml kg^{-1} body weight.

Animals were observed at least twice daily to monitor for disease signs, and animals that survived to day 28 were deemed to be protected. Study personnel alleviated unnecessary suffering of infected animals by euthanizing clinically moribund animals. The criteria used as the basis for euthanasia of moribund animals were defined before study initiation and included magnitude of responsiveness, reduced body temperature, and/or specified alterations to serum chemistry parameters[35]. Serum chemistry was analysed using a Vitros 350 Chemistry System (Ortho Clinical Diagnostics), and coagulation parameters were evaluated using a Sysmex CA-1500 coagulation analyser (Siemens Healthcare Diagnostics). Haematology analysis was conducted using a Siemens Advia 120 Hematology System with multispecies software (Siemens Healthcare Diagnostics). On days in which GS-5734 or vehicle dosing were scheduled with blood sample collection for clinical pathology or viraemia analysis, blood samples were collected immediately before dose administration.

Viral genomic sequence analysis. Analysis of viral genomic sequence was conducted with the purpose of evaluating genomic sequence change patterns consistent with development of resistance against GS-5734. Attempts were made to obtain

sequence of RNA-dependent RNA polymerase gene (*L*) of Ebola virus from all EBOV-RNA-positive rhesus monkey plasma samples obtained during the efficacy studies. Deep sequencing screening of the *L* gene was completed using previously described methods[36,37]. Mutations and large subclonal events (≥10% of population) were reviewed for: non-synonymous substitutions in treated animals that succumbed to infection, any substitution enriched in treated populations regardless of survival status, and clusters of substitutions in any treated animal.

cDNA synthesis was performed using Superscript III First-Strand Synthesis System (Invitrogen). cDNA was amplified with Phusion Hot Start Flex DNA Polymerase (New England Biolabs) using overlapping 1,500-kb amplicons (primer information available upon request). After pooling and purification with AMPure XP Reagent (Beckman Coulter), PCR products were fragmented using the Covaris S2 instrument (Covaris). Libraries were prepared with the Illumina TruSeq DNA Sample Preparation kit (Illumina) on the Caliper ScicloneG3 Liquid Handling Station (PerkinElmer). After measurement by real-time PCR with the KAPA qPCR Kit (Kapa Biosystems), libraries were diluted to 4 or 10 nM. Cluster amplification was performed on the Illumina cBot, and libraries were sequenced on the Illumina Nextseq or Illumina HiSeq 2500 using the 150 or 100 bp paired-end format. Viral assemblies were completed in DNAStar Lasergene nGen. Amplification primer removal, quality trimming, and trim-to-mer were performed on reads with a minimum similarity to the reference of 93% (four-base mismatch). A target depth of 1,200 is sought and single nucleotide polymorphisms at positions with fewer than 200 read depth were removed from the analysis. A consensus change was defined as a change relative to the deposited EBOV sequence (GenBank: AY354458) present in ≥50% of the population. Below that threshold, single nucleotide polymorphisms were considered subclonal substitutions and part of a minority subpopulation of the virus. Consensus sequence for the region covered in this screening is available in GenBank and the accession numbers are provided in Extended Data Table 5.

Animal care. Pharmacokinetic and radiolabelled tissue distribution studies in uninfected cynomolgus and rhesus macaques were conducted at Covance, Inc. Protocols were reviewed by an Institutional Animal Care and Use Committee (IACUC) at Covance. Efficacy experiments involving EBOV were performed in animal biosafety level 4 (ABSL-4) at USAMRIID. Research was conducted under an Institutional Animal Care and Use Committee approved protocol in compliance with the Animal Welfare Act, PHS Policy, and other federal statutes and regulations relating to animals and experiments involving animals. The facilities where this research was conducted are accredited by the Association for Assessment and Accreditation of Laboratory Animal Care, International and strictly adhere to principles stated in the Guide for the Care and Use of Laboratory Animals, National Research Council, 2011 (National Academies Press, Washington, DC).

Statistics. Combined vehicle group from part 1 and 2 ($n = 6$ animals total) was used as control group in all statistical comparisons of GS-5734 efficacy evaluations. The impact of GS-5734 treatment on the survival rates was estimated using Kaplan–Meier method and analysed by log-rank analysis using Dunnett–Hsu procedure to adjust for multiple comparisons. The effect on systemic viral RNA levels was assessed by analysis of variance (ANOVA), comparing each GS-5734 treatment group with vehicle group using Dunnett's test to adjust for multiple comparisons. Wilcoxon rank-sum test without adjustment for multiple comparisons was used to compare the effects of GS-5734 treatment on haematology, coagulation, and clinical chemistry parameters. All data met the statistical assumptions of the test performed.

26. Uebelhoer, L. S. *et al.* High-throughput, luciferase-based reverse genetics systems for identifying inhibitors of Marburg and Ebola viruses. *Antiviral Res.* **106,** 86–94 (2014).
27. Towner, J. S. *et al.* Generation of eGFP expressing recombinant Zaire Ebolavirus for analysis of early pathogenesis events and high-throughput antiviral drug screening. *Virology* **332,** 20–27 (2005).
28. Shao, R. & Guo, X. Human microvascular endothelial cells immortalized with human telomerase catalytic protein: a model for the study of in vitro angiogenesis. *Biochem. Biophys. Res. Commun.* **321,** 788–794 (2004).
29. Mason, S. W. *et al.* Polyadenylation-dependent screening assay for respiratory syncytial virus RNA transcriptase activity and identification of an inhibitor. *Nucleic Acids Res.* **32,** 4758–4767 (2004).
30. Durand-Gasselin, L. *et al.* Nucleotide analogue prodrug tenofovir disoproxil enhances lymphoid cell loading following oral administration in monkeys. *Mol. Pharm.* **6,** 1145–1151 (2009).
31. Noton, S. L., Deflube, L. R., Tremaglio, C. Z. & Fearns, R. The respiratory syncytial virus polymerase has multiple RNA synthesis activities at the promoter. *PLoS Pathog.* **8,** e1002980 (2012).
32. Noton, S. L. *et al.* Respiratory syncytial virus inhibitor AZ-27 differentially inhibits different polymerase activities at the promoter. *J. Virol.* **89,** 7786–7798 (2015).
33. Tremaglio, C. Z., Noton, S. L., Deflube, L. R. & Fearns, R. Respiratory syncytial virus polymerase can initiate transcription from position 3 of the leader promoter. *J. Virol.* **87,** 3196–3207 (2013).
34. Lodeiro, M. F. *et al.* Identification of multiple rate-limiting steps during the human mitochondrial transcription cycle in vitro. *J. Biol. Chem.* **285,** 16387–16402 (2010).
35. Warren, T. K. *et al.* Euthanasia assessment in Ebola virus infected nonhuman primates. *Viruses* **6,** 4666–4682 (2014).
36. Kugelman, J. R. *et al.* Emergence of Ebola Virus escape variants in infected nonhuman primates treated with the MB-003 antibody cocktail. *Cell Rep.* **12,** 2111–2120 (2015).
37. Kugelman, J. R. *et al.* Ebola virus genome plasticity as a marker of its passaging history: a comparison of in vitro passaging to non-human primate infection. *PLoS ONE* **7,** e50316 (2012).
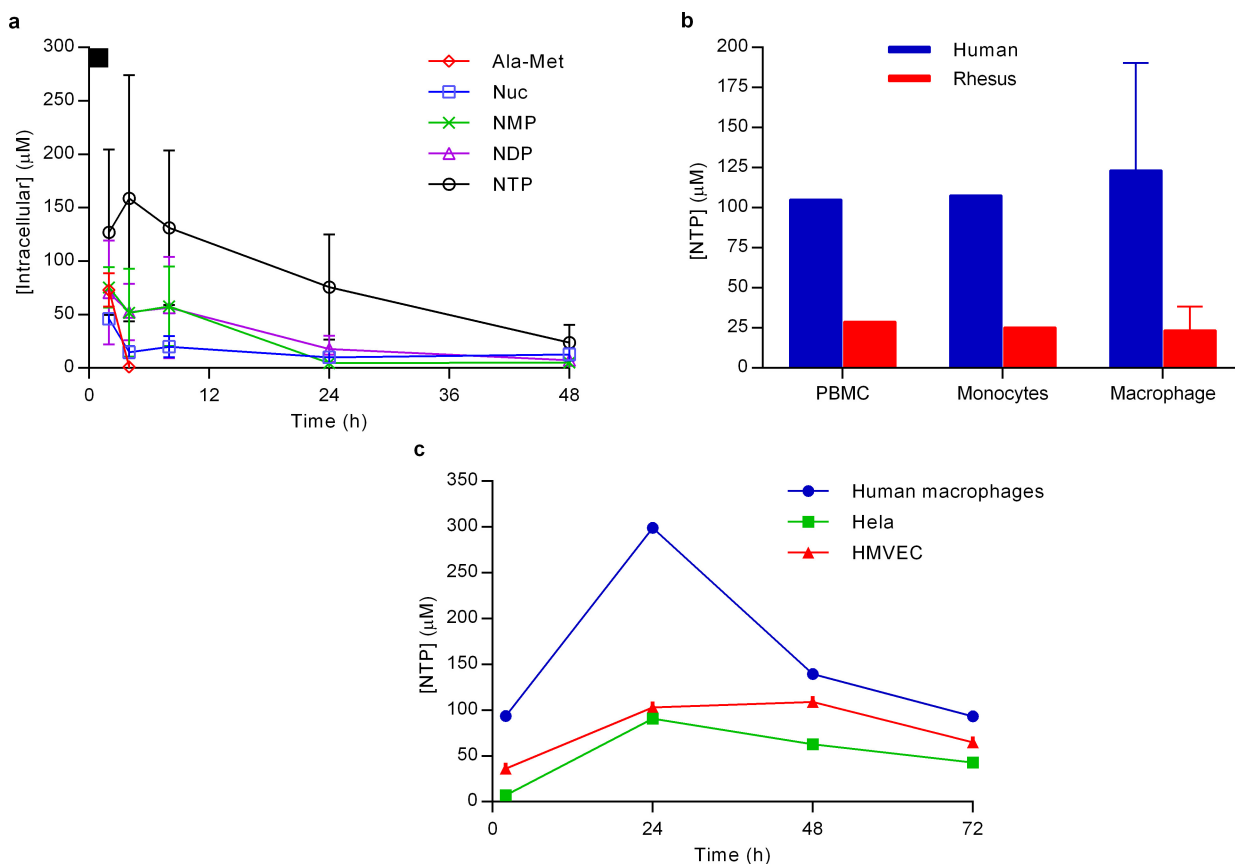
Extended Data Figure 1 | Intracellular metabolism of GS-5734.
a, Intracellular metabolite profile in human macrophages. Following a 2-h
pulse incubation (black bar at top of y axis) of human monocyte-derived
macrophages with 1 μM GS-5734 (mean ± s.d., from three donors).
GS-5734 is rapidly metabolized and not detected in cells. Transient
exposure to the intermediate alanine metabolite (Ala-Met) is observed,
followed by persistent Nuc exposure. The pharmacologically active NTP
is formed quickly, achieving a maximum intracellular concentration at 4 h
and persisted with a half-life of 16 ± 1 h in the three donors. Intracellular
concentration was estimated on the basis of an intracellular volume of
1 pl per cell. **b**, Efficiency of GS-5734 activation in human and rhesus
cells *in vitro*. Intracellular NTP concentrations formed in human and
rhesus PBMCs, monocytes, and monocyte-derived macrophages during
a 2-h incubation with 1 μM GS-5734 (results are the mean ± s.d. of two

(PBMC and monocyte) to six (macrophage) independent experiments
performed with cells from different donors). Intracellular concentrations
were estimated on the basis of a cell volume of 0.2 pl per cell for PBMCs
and monocytes and 1 pl per cell for macrophages. **c**, Intracellular NTP
levels required for inhibition of EBOV replication in cell culture. The
mixture of GS-5734 and its diastereomer on phosphorous was incubated
continuously for 72 h at 1 μM and levels of intracellular NTP were
determined (results are the average of duplicate incubations performed
in each cell type; two independent studies were performed in HMVEC
isolated from different donors). The corresponding EBOV EC_{50} values for
the prodrug diastereomeric mixture were 100, 184, and 121 nM in human
macrophages, HeLa, and HMVEC, respectively, suggesting that an average
intracellular NTP concentration of approximately 5 μM is required for 50%
inhibition of EBOV *in vitro*.
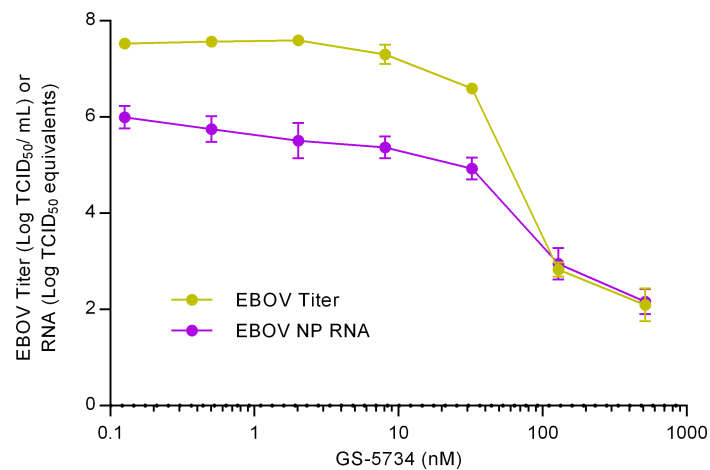
Extended Data Figure 2 | Inhibition of EBOV Makona replication by GS-5734. Huh-7 cells infected with wild-type EBOV (Makona) were incubated for 3 days in the presence of serial dilutions of GS-5734. The amount of infectious virus produced was quantified by endpoint dilution assay of culture media on fresh Vero cell monolayers and the tissue culture infectious dose that caused 50% infection ($TCID_{50}$) was determined. Independently, total RNA was extracted from infected cells and EBOV RNA levels were quantified using a nucleoprotein (NP) gene-specific qRT–PCR. Values represent mean ± s.d. of log_{10}-transformed values, $n = 4$ replicates.
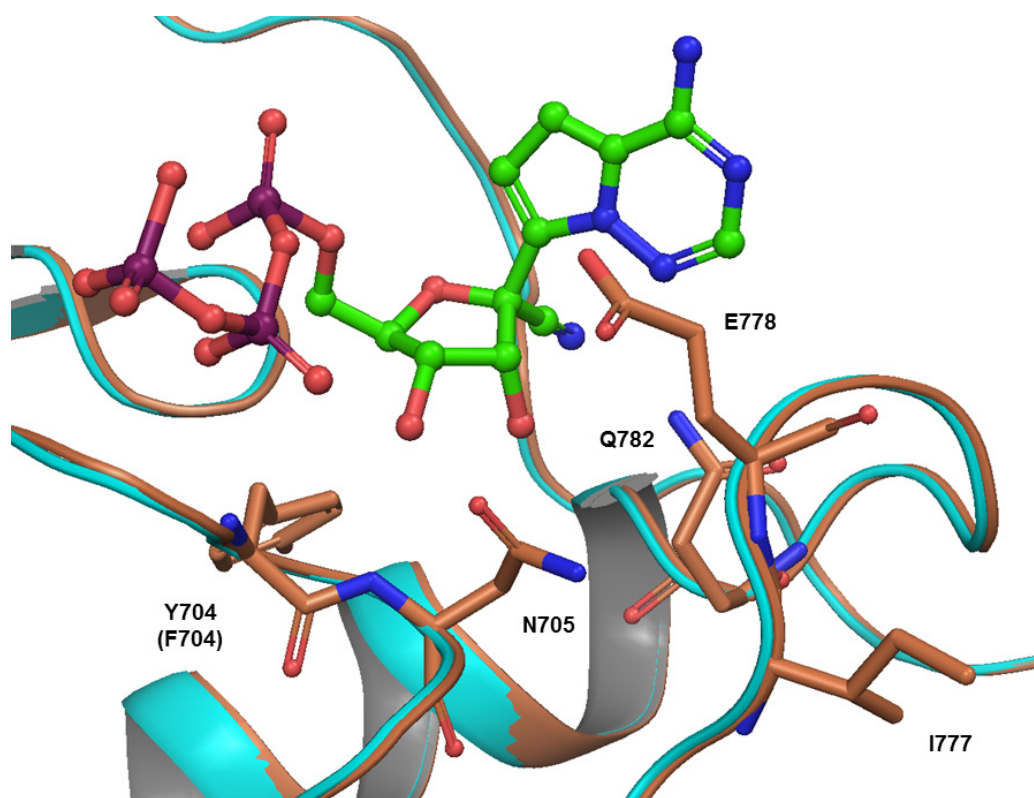
Extended Data Figure 3 | Homology model of RSV A2 (cyan) and EBOV (coral) polymerase based on HIV reverse transcriptase (PDB: 1RTD) with NTP (green and red representing the nucleoside and triphosphate portion, respectively).

Extended Data Figure 4 | Clinical signs of disease in individual rhesus monkeys exposed to Ebola virus. Animals were observed multiple times each day and were subjectively assigned a clinical disease score ranging from 0 to 5 based on responsiveness, posture, and activity. Maximum daily scores were converted to colour code, with darker colours indicative of more severe disease signs. The schematic was truncated to emphasize clinical scores during the acute disease phase, and none of the animals exhibited clinical disease signs outside of the times that are shown.
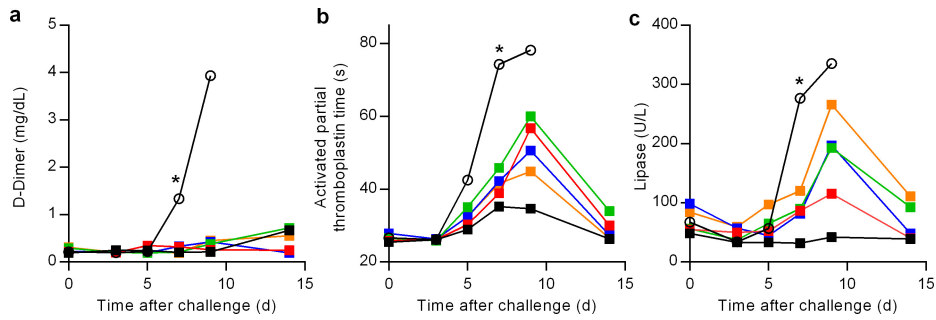
Extended Data Figure 5 | Amelioration of EVD clinical pathology by GS-5734 in rhesus monkeys. a–c, Group mean ($n = 6$ per group) values of D-dimer (**a**), activated partial thromboplastin time (**b**), and lipase (**c**). Black (open symbols), vehicle; red, $3 \, \mathrm{mg \, kg^{-1}}$ d0; green, $3 \, \mathrm{mg \, kg^{-1}}$ d2; blue, $10/3 \, \mathrm{mg \, kg^{-1}}$ d2; orange, $10/3 \, \mathrm{mg \, kg^{-1}}$ d3; black (closed symbols), $10 \, \mathrm{mg \, kg^{-1}}$ d3. Error bars omitted for clarity; x axes truncated at day 15. *$P < 0.05$ for comparison of mean change from d0 of vehicle and $10 \, \mathrm{mg \, kg^{-1}}$ d3 groups at day 7.

Extended Data Table 1 | *In vitro* **cytotoxicity of GS-5734 and Nuc in human cell lines and primary cells**

	CC$_{50}$ (µM)*		
	GS-5734	Nuc	Puromycin
Human cell lines			
HEp-2	6.0 ± 1.5	> 100	0.53 ± 0.10
HepG2	3.7 ± 0.2	> 100	0.73 ± 0.01
PC-3	8.9 ± 1.6	> 100	0.52 ± 0.11
MT-4	1.7 ± 0.4	69.3 ± 25.7	0.12 ± 0.03
Human primary cells			
Hepatocytes	2.5 ± 0.6	> 100	1.5 ± 0.6
Renal proximal tubular epithelial cells (RPTEC)	12.9 ± 6.2	> 100	1.1 ± 0.3
Quiescent PBMCs	> 20	> 100	6.8 ± 1.4
Stimulated PBMCs	14.8 ± 5.8	> 100	1.6 ± 0.2

*Drug concentrations reducing the cell viability by 50% (CC$_{50}$) are presented. All CC$_{50}$ values represent the mean ± s.d. of at least two independent experiments. Puromycin was included in experiments as a positive control for cytotoxicity.

Extended Data Table 2 | Individual plasma viral RNA ($\log_{10}$(copies ml^{-1}))

Treatment Description	Animal #	Plasma Viral RNA on Study Day														
		0	2	3	4	5	6	7	8	9	10	12	14	18	21/22	28/29
Vehicle																
	1	ND	ND	ND	6.6	9.0	–	10.0	–	9.5						
	2	ND	ND	ND	5.9	8.9	–	9.8								
	3	ND	ND	6.5	8.2	8.5	–	8.6								
	4	ND	ND	DET	6.6	8.4	–	8.4	–	8.1						
	5	ND	ND	5.8	8.8	10.0	10.3									
	6	ND	ND	5.4	7.4	9.4	–	9.2	8.7							
GS-5734 3 mg/kg D0																
	1	ND	ND	ND	DET	6.0	–	7.3	–	7.4	7.3					
	2	ND	ND	ND	ND	4.9	–	6.8	–	9.9						
	3	ND	ND	ND	DET	5.5	–	6.5	–	5.8	–	DET	ND	–	ND	ND
	4	ND	ND	ND	ND	4.9	–	5.8	–	5.6	–	DET	ND	–	ND	ND
	5	ND	ND	ND	DET	5.7	–	9.1	–	9.1	8.6					
	6	ND	ND	DET	7.2	9.3	–									
GS-5734 3 mg/kg D2																
	1	ND	ND	ND	DET	6.0	–	6.6	–	6.8	–	6.9	6.0	–	ND	ND
	2	ND	ND	ND	6.4	7.6	–	7.1	–	6.8	–	DET	ND	ND		
	3	ND	ND	ND	DET	6.6	–	7.5	–	8.2	–	5.2	ND	–	ND	ND
	4	ND	ND	ND	5.1	7.0	–	7.4	–	6.6	–					
	5	ND	ND	4.9	6.9	8.1	–	8.1	–	6.6	–	5.2	ND	–	ND	ND
	6	ND	ND	ND	DET	5.5	–	6.7	–	5.9	–	ND	ND	–	ND	ND
GS-5734 10/3 mg/kg D2																
	1	ND	DET	5.2	5.8	7.9	–	8.2	–	8.0						
	2	ND	ND	ND	ND	DET	–	DET	–	ND	–	ND	ND	–	ND	ND
	3	ND	ND	ND	DET	6.1	–	7.8	–	7.5						
	4	ND	ND	ND	4.9	5.5	–	6.1	–	DET	–	ND	ND	–	ND	ND
	5	ND	ND	ND	ND	DET	–	8.2	–	8.2						
	6	ND	ND	ND	5.3	7.1	–	6.9	8.1							
GS-5734 10/3 mg/kg D3																
	1	ND	ND	DET	5.4	6.5	–	6.5	–	5.0	–	ND	ND	–	ND	ND
	2	ND	ND	5.3	6.2	7.1	–	6.8	–	6.0	–	ND	ND	–	ND	ND
	3	ND	ND	DET	5.1	6.9	–	7.0	–	7.0	–	6.7	ND	–	ND	ND
	4	ND	ND	ND	DET	7.0	–	8.1	–	8.3	–	6.2	DET	–	ND	ND
	5	ND	ND	ND	ND	DET	–	ND	–	5.5	–	ND	ND	–	ND	ND
	6	ND	ND	DET	5.8	6.6	–	6.2	–	6.8	–	ND	ND	–	ND	ND
GS-5734 10 mg/kg D3																
	1	ND	ND	DET	5.7	6.1	–	6.0	–	DET	–	ND	ND	–	ND	ND
	2	ND	ND	ND	DET	DET	–	DET	–	5.6	–	ND	ND	–	ND	ND
	3	ND	ND	ND	6.7	DET	–	ND	–	ND	–	ND	ND	–	ND	ND
	4	ND	ND	ND	ND	DET	–	ND	–	ND	–	ND	ND	–	ND	ND
	5	ND	ND	ND	ND	ND	–	ND	–	ND	–	ND	ND	–	ND	ND
	6	ND	ND	DET	5.6	6.9	–	5.5	–	5.9	–	ND	ND	–	ND	ND

–, sample not collected (days 6, 8, 10, and 18 were unscheduled samplings of succumbed animals only). DET, detectable, but below the lower limit of quantitation (8.0×10^4 copies ml^{-1}); ND, not detected, that is, below limit of detection.

Extended Data Table 3 | Summary and statistical analysis of plasma viral RNA

Day	Vehicle	GS-5734 3 mg/kg D0	GS-5734 3 mg/kg D2	GS-5734 10/3 mg/kg D2	GS-5734 10/3 mg/kg D3	GS-5734 10 mg/kg D3
		Plasma Viral RNA, mean $\log_{10}$ copies ml^{-1} (P value*)				
3	4.77	3.32 (**0.019**)	3.32 (**0.020**)	3.36 (**0.023**)	4.33 (0.454)	3.63 (0.062)
4	7.24	4.66 (**0.001**)	5.52 (**0.024**)	4.49 (**0.001**)	5.06 (**0.005**)	4.81 (**0.002**)
5	9.05	6.04 (**<0.001**)	6.82 (**0.002**)	6.07 (**<0.001**)	6.52 (**0.001**)	5.12 (**<0.001**)
7	9.19	7.09 (**0.013**)	7.24 (**0.015**)	7.00 (**0.007**)	6.28 (**0.001**)	4.24 (**<0.001**)
9	8.76	7.55 (0.351)	6.82 (0.132)	6.30 (0.065)	6.42 (0.072)	4.22 (**0.001**)
12	–	4.90 (NA)	5.05 (NA)	3.00 (NA)	4.14 (NA)	3.00 (NA)

*P values are from ANOVA comparing each GS-5734 treatment group with vehicle group using Dunnett's test to adjust for multiple comparisons ($n = 6$ animals per group, PCR sample assays performed in triplicate). EBOV RNA values reported as '<LOD' were substituted as 10^3 RNA copies ml^{-1}, and values reported as '>LOD, <LLOQ' were substituted as LLOQ of 8.0×10^4 RNA copies ml^{-1} for computation purpose. Statistically significant P values ($P < 0.05$) are highlighted in bold. NA, not applicable, owing to no survivors in vehicle group.

Extended Data Table 4 | Statistical summary of selected clinical pathology parameters

Parameter	Vehicle	GS-5734 3 mg/kg D0	GS-5734 3 mg/kg D2	GS-5734 10/3 mg/kg D2	GS-5734 10/3 mg/kg D3	GS-5734 10 mg/kg D3
Platelet count (10^3/ µL)	-279	-118 (**0.012**)	-202 (0.055)	-155 (0.055)	-98 (**0.014**)	-65 (**0.008**)
PT (sec)	5.0	1.3 (**0.01**)	3.2 (0.27)	1.6 (0.06)	2.5 (**0.02**)	1.7 (**0.01**)
APTT (sec)	47.7	12.6 (**0.012**)	19.3 (**0.014**)	14.3 (**0.008**)	15.2 (**0.008**)	9.8 (**0.008**)
Fibrinogen (mg/dL)	2.5	-4.7 (**0.012**)	-5.5 (**0.008**)	-5.0 (**0.014**)	-5.0 (**0.014**)	-4.4 (**0.008**)
TT (sec)	50.2	-1.4 (**0.012**)	2.6 (**0.008**)	1.4 (**0.008**)	3.6 (**0.008**)	-1.5 (**0.008**)
Antithrombin (%)	-39.6	-6.1 (**0.012**)	-10.3 (**0.008**)	-7.9 (**0.008**)	5.6 (**0.008**)	3.1 (**0.008**)
D-dimer (mg/dL)	1.15	0.13 (**0.012**)	-0.09 (**0.008**)	0.11 (**0.008**)	-0.12 (**0.005**)	0.02 (**0.007**)
ALT (U/L)	340	14 (**0.012**)	24 (**0.008**)	116 (0.083)	28 (**0.008**)	32 (**0.008**)
AST (U/L)	1425	273 (**0.014**)	206 (**0.014**)	90 (**0.020**)	157 (**0.014**)	36 (**0.014**)
ALP (U/L)	1238	-69 (**0.012**)	-74 (**0.008**)	7 (**0.008**)	8 (**0.008**)	-66 (**0.008**)
CRK (U/L)	5420	1277 (**0.020**)	1002 (**0.014**)	841 (**0.014**)	682 (**0.014**)	96 (**0.014**)
GGT (U/L)	146	-12 (**0.012**)	-13 (**0.008**)	-2 (**0.008**)	1 (**0.008**)	-12 (**0.008**)
LDH (U/L)	8391	1006 (**0.020**)	2263 (**0.014**)	2358 (**0.014**)	2439 (**0.014**)	352 (**0.014**)
Bilirubin (mg/dL)	1.3	0 (0.071)	0 (**0.048**)	0 (**0.048**)	0 (**0.048**)	0 (**0.048**)
BUN (mg/dL)	60	0 (**0.021**)	1 (**0.028**)	2 (**0.036**)	5 (0.055)	1 (**0.021**)
Creatinine (mg/dL)	1.80	0.12 (**0.015**)	0.27 (**0.017**)	0.18 (**0.014**)	0.27 (**0.014**)	0.43 (0.066)
Lipase (U/L)	205	17 (0.14)	34 (0.12)	-17 (0.055)	36 (0.12)	-12 (**0.036**)
Triglycerides (mg/dL)	538	-7 (**0.012**)	52 (**0.008**)	63 (**0.008**)	420 (0.083)	-6 (**0.008**)
CRP (mg/dL)	48.6	48.8 (0.83)	43.8 (1.0)	41.2 (0.31)	35.3 (0.24)	13.2 (**0.008**)
Albumin (g/dL)	-1.5	-0.8 (**0.012**)	-1.2 (0.170)	-0.8 (**0.036**)	-0.8 (**0.022**)	-0.7 (**0.008**)
Total protein (mg/dL)	-1.1	-0.5 (**0.034**)	-0.9 (0.27)	-0.6 (0.17)	-0.4 (**0.035**)	-0.4 (**0.008**)
Chloride (mEq/dL)	-14	-3 (**0.011**)	-5 (**0.008**)	-6 (**0.013**)	-6 (0.067)	0 (**0.008**)
Phosphate (mEq/dL)	0.2	-2.1 (**0.036**)	-2.5 (**0.021**)	-1.5 (0.12)	-1.0 (0.65)	-0.3 (0.93)
Sodium (mg/dL)	-17	-8 (**0.019**)	-10 (**0.042**)	-9 (0.054)	-7 (**0.042**)	-5 (**0.014**)

*Wilcoxon rank-sum test without adjustment for multiple comparisons using a combined vehicle group as a control group for the analysis ($n = 6$ animals per group). Statistically significant P values ($P < 0.05$) are highlighted in bold.
ALP, alkaline phosphatase; ALT, alanine aminotransferase; APTT, activated partial thromboplastin time; AST, aspartate aminotransferase; BUN, blood urea nitrogen; CRK, creatine kinase; CRP, C-reactive protein; GGT, gamma glutamyl transferase; LDH, lactate dehydrogenase; PT, prothrombin time; TT, thrombin time.

Extended Data Table 5 | *L* gene deep sequencing screening sample description and metrics

Treatment Description	Animal #	Day	Survival Outcome	Genbank Accession Number	% *L* Gene Coverage	Polymerase Amino Acid and Codon Changes	% of Population with Change	iSNV Description
Vehicle	6	7	Deceased	KU321182	100.0	W (TGG) @191 (T+G)	21.9	Volatile sub clonal substitution observed in most samples in all treatment groups and controls >2% of population. Causes a frameshifting insertion at the end of a large homopolymer.
3 mg/kg D0	2	7	Deceased	KU321189	100.0	E (GAA) @2173 E (GAg)	99.5	Synonymous substitution unlikely selection pressure.
3 mg/kg D0	6	5	Deceased	KU321084	100.0	G (GGT) @1160 G (GGc)	44.5	Synonymous substitution unlikely selection pressure.
3 mg/kg D2	1	7	Survived	KU321152	100.0	W (TGG) @191 (T+G)	21.8	Volatile sub clonal substitution observed in most samples in all treatment groups and controls >2% of population. Causes a frameshifting insertion at the end of a large homopolymer.
						Q (CAA) @805 (+AA)	26.6	Volatile sub clonal substitution observed in most samples in all treatment groups and controls >2% of population. Causes a frameshifting insertion at the end of a large homopolymer.
3 mg/kg D2	1	9	Survived	KU321162	100.0	W (TGG) @191 (T+G)	13.8	Volatile sub clonal substitution observed in most samples in all treatment groups and controls > 2% of population. Causes a frameshifting insertion at the end of a large homopolymer.
3 mg/kg D2	3	5	Survived	KU321165	100.0	W (TGG) @191 (T+G)	23.4	Volatile sub clonal substitution observed in most samples in all treatment groups and controls >2% of population. Causes a frameshifting insertion at the end of a large homopolymer.
						Q (CAA) @1755 Q (CAG)	99.0	Synonymous mutation unlikely selection pressure.
3 mg/kg D2	4	9	Deceased	KU321088	100.0	W (TGG) @191 (T+G)	13.9	Volatile sub clonal substitution observed in most samples in all treatment groups and controls >2% of population. Causes a frameshifting insertion at the end of a large homopolymer.
10/3 mg/kg D2	3	5	Deceased	KU321098	81.2	—	24.2	Non-coding substitution, unlikely selection pressure.
10/3 mg/kg D3	2	9	Survived	KU321149	100.0	K (AAG) @341 K (AAa)	26.7	Synonymous substitution unlikely selection pressure.
						I (ATC) @348 S (AgC)	22.3	Non-synonymous substitution tolerated by survivor.
10/3 mg/kg D3	3	7	Survived	KU321172	99.3	K (AAA) @1387 K (AAg)	28.3	Synonymous substitution unlikely selection pressure.
						F (TTT) @1827 (TT-)	20.6	Indel causes a frameshifting deletion at the end of a large homopolymer region.
10 mg/kg D3	1	5	Survived	KU321154	86.5	K (AAG) @659 N (AAt)	28.0	Non-synonymous substitution tolerated by survivor.
						Q (CAA) @805 (+AA)	40.2	Volatile sub clonal substitution observed in most samples in all treatment groups and controls >2% of population. Causes a frameshifting insertion at the end of a large homopolymer.

Genomic sequence analysis was conducted on all samples containing quantifiable concentrations of viral RNA (that is, >LLOQ as assessed by quantitative real-time PCR).
Sequences for which no change (defined as >2% of the population) was noted from the reference sequence are not shown.
iSNV, intra-host Single Nucleotide Variant.